

Simultaneous Photoionization and Photoexcitation of Helium[†]

Robert L. Brown

National Radio Astronomy Observatory, * Green Bank, West Virginia 24944

(Received 2 October 1969)

A general method is presented for calculating the f values for all permitted dipole transitions involving simultaneous photoionization and photoexcitation of helium. The cross section for ions excited into the $n=2$ state is compared with experiment and with a similar calculation by Salpeter and Zaidi; their result, that the ejected electron is in a p state is confirmed. The probability for the residual He^+ ion to be excited to a state of principle quantum number n is evaluated for $n=2-10$, and the probability for the photoelectron to be in a p state is compared with the probability for it to be emitted in an s state. It is found that the inclusion of contributions from simultaneous photoionization and photoexcitation, and from double ionization in the total helium photoionization cross section, improves the agreement between theory and the experimental data at high energies.

I. INTRODUCTION

Recent measurements of the helium photoionization cross section made with a photoelectron spectrometer allow the cross section for double excitation (bound free) to be separated from that for ordinary photoionization, where the residual ion remains in the ground state.¹ These results have renewed interest in calculations of the helium photoionization cross section in which such double excitation contributions are explicitly included.²

The first theoretical investigations of the helium photoionization cross section were conducted nearly 40 years ago^{3, 4} and have since been reconsidered with increasingly accurate wave functions used for both the bound and free states: The agreement with experiment is now quite good, especially near threshold.⁵⁻⁷ However, these calculations were made under the assumption that the ejected electron negligibly disturbs the bound electron leaving it in the $1s$ state of the ion. For photon energies greater than ~ 65.4 eV (threshold for the $n=2$ state of the ion), transitions are possible to doubly excited (bound-free) states, and for energies greater than ~ 79 eV, excitation of the remaining electron to the continuum of the ion (double ionization) becomes accessible; and these contributions must be included in the total photoionization cross section before comparison with experiment is meaningful.

The purpose of this paper is to describe a general method for evaluating the oscillator strengths for simultaneous photoionization and photoexcitation of helium and to compare these results with recent data. Section II outlines a general method used to calculate the cross sections due to double excitation (bound free); Sec. III is a statement of the theoretical results and a comparison with experiment; and Sec. IV is a summary of the helium photoionization cross section including the effects of double excitation.

II. GENERAL APPROACH

Although Dalgarno and Stewart⁷ and Salpeter and Zaidi⁵ (SZ) have calculated the oscillator strength for one transition involving simultaneous photoexcitation and photoionization of helium, $1s^2 - (2s, \epsilon p)^1 P$; their method, applicable only for transitions to $(ns, \epsilon p)^1 P$ states, used an 18-parameter Hylleraas wave function for the bound state of helium and the Hartree approximation for the free state, and thus does not easily lend itself to direct extension for the evaluation of oscillator strengths for other permitted dipole transitions. However, a general approach can be effected if the ground state is represented by the wave function introduced by Byron and Joachain,^{8, 9} which is an expansion of the bound state in relative partial waves:

$$\Psi_b(\vec{r}_1, \vec{r}_2) = \frac{1}{4\pi} \sum_l F_l(\vec{r}_1, \vec{r}_2) P_l(\cos\theta_{12}) , \tag{1}$$

$$F_l(\vec{r}_1, \vec{r}_2) = \sum_{p \leq q} A_{pq}^{(l)} r_1^l r_2^l (r_1^p r_2^q + r_1^q r_2^p) e^{-\beta(r_1+r_2)/2} .$$

The Legendre function can also be expanded:

$$P_l(\cos\theta_{12}) = \sum_{m=-l}^l \frac{(l-|m|)!}{(l+|m|)!} P_l^m(\cos\theta_1) P_l^m(\cos\theta_2) e^{im(\phi_1 - \phi_2)} .$$

The advantage of the Byron-Joachain (BJ) wave function over the Hylleraas type is that the latter involves interelectronic r_{12} terms which tend to severely complicate calculations. However, the 18-parameter Hylleraas wave function as used by SZ does give a much better ground-state energy than does the BJ wave function in spite of the fact that the latter uses 15 parameters in each of three partial waves: -2.903716 and -2.9020 a. u. , respectively.

The final state of the continuum electron and hydrogenic ion has been represented by a symmetrized product:

$$\Psi_f(\vec{r}_1, \vec{r}_2) = 2^{-1/2} [R_{nl}(r_1) Y_{lm}(\Omega_1) R_{\epsilon, \lambda}(r_2) Y_{\lambda, -m}(\Omega_2) + (2 \leftrightarrow 1)] , \quad (2)$$

where the radial wave functions $R_{nl}(r)$ and $R_{\epsilon, \lambda}(r)$ are eigenfunctions of

$$\left(\frac{d^2}{dr^2} - \frac{l(l+1)}{r^2} + \frac{2Z}{r} + \left\{ \frac{-Z^2/n^2}{\epsilon} \right\} \right) \begin{Bmatrix} R_{nl}(r) \\ R_{\epsilon\lambda}(r) \end{Bmatrix} = 0 ,$$

where ϵ is the energy of the photoelectron, $h\nu = \text{ionization potential} + \epsilon$.¹⁰

$R_{nl}(r)$ is the bound-state wave function for a hydrogenic ion of nuclear charge $Z=2$ which has the form¹¹

$$R_{nl}(r) = \frac{1}{(2l+1)!} \left(\frac{(n+l)!}{2n(n-l-1)!} \right)^{1/2} \left(\frac{2Z}{n} \right)^{3/2} e^{-Zr/n} \left(\frac{2Zr}{n} \right) {}_1F_1\left(- (n-l-1), 2l+2, \frac{2Zr}{n}\right) ; \quad (3)$$

and the continuum electron is represented by a completely screened Coulomb wave function which can be conveniently expressed as an integral:

$$R_{\epsilon, \lambda}(r) = (-1)^{\lambda+1} 2 \prod_{s=1}^{\lambda+1} (s^2 + n_0^2)^{1/2} (1 - e^{-2\pi n_0})^{-1/2} \frac{1}{(2kr)^{\lambda+1}} \frac{1}{2\pi} \\ \times \oint e^{-2ikr\xi} (\xi + \frac{1}{2})^{-in_0 - \lambda - 1} (\xi - \frac{1}{2})^{in_0 - \lambda - 1} d\xi , \quad (4)$$

where $n_0 = Z/k$ and $k^2 = \epsilon$.

Cross sections for simultaneous photoionization and photoexcitation in helium are then readily calculable by employing the dipole momentum matrix element:

$$\sigma = \frac{4\pi^2 \alpha a_0^2}{\hbar \omega} \int d\epsilon \left| \langle \Psi_f(\vec{r}_1, \vec{r}_2) \left| \frac{\partial}{\partial z} + \frac{\partial}{\partial z_2} \right| \Psi_b(\vec{r}_1, \vec{r}_2) \rangle \right|^2 \delta[\hbar\omega - I(n, l) - \epsilon] , \quad (5)$$

using (1) for the bound state and (2)–(4) to describe the free state. Transitions from the ground state to any allowed excited state of the residual ion can be evaluated by using the appropriate (n, l) in (3) and (5). Without dwelling unnecessarily on the details of this calculation, it should be noted that the angular integrals in the matrix element give a condition on λ , $\lambda = l \pm 1$. This, of course, is a statement of the Laporte rule and determines whether transitions from $1s^2$ go to $(ns, \epsilon p)^1P$ or to $(np, \epsilon s)^1P$. The remaining radial integrals are

$$\int_0^\infty e^{-(\beta/2 + Z/n)r} r {}_1F_1\left(- (n-l-1), 2l+2, \frac{2Zr}{n}\right) dr_1 , \\ \int_0^\infty e^{-\beta/2r_2} r_2 {}_1F_1\left(- (n-l-1), 2l+2, \frac{2Zr_2}{n}\right) dr_2 \frac{1}{2\pi} \oint e^{-2ikr_2\xi} (\xi + \frac{1}{2})^{-in_0 - l - 1} (\xi - \frac{1}{2})^{in_0 - l - 1} d\xi .$$

The procedure for integrating over r_2 has been described previously in terms of a sum of residues,¹² or equivalently it has been shown by Gordon¹³ and by others¹⁴ that the solution can be expressed as a sum of hypergeometric functions. The integral over r_1 is straightforward:

$$\frac{\Gamma(s+1)}{(Z/n + \frac{1}{2}\beta)^{s+1}} {}_2F_1\left(- (n-l-1), s+1; 2l+2; \frac{2Z}{n(Z/n + \frac{1}{2}\beta)}\right) .$$

Following this procedure, the cross sections may be evaluated in closed form for photoionization with simultaneous photoexcitation to any permitted state (n, l) of the ion.

III. CROSS SECTIONS

Application of the general approach outlined above to transitions from the ground $1s^2$ state of helium to the allowed excited states of the ion ($n \leq 10$) has produced the following results.

1. Transition $1s^2 - (1s, \epsilon p)^1P$.

Although these transitions, which leave the ion in its ground state, have been considered in detail elsewhere,⁴⁻⁷ it is nevertheless useful to repeat this calculation for the case when the bound state is represented by the BJ wave function (1). The continuum oscillator strengths $df/d\epsilon$ have been calculated using the momentum matrix element (5), the free state (2)–(4) with $(n, l) = (1, 0)$ in (3), and the results are tabulated as a function of excitation energy in the second column of Table I.

A comparison with the results of similar calculations reveals that the f values obtained from this formulation are smaller than those obtained by SZ near the spectral head but that they are $\sim 10\%$ larger at higher energies. Further, the present results lie 5–10% higher than those of Bell and

Kingston,⁶ who used a 20-parameter Hylleraas bound-state wave function and a polarized orbital continuum wave function, whereas SZ's results are $\sim 10\%$ lower than those of Bell and Kingston (except at the spectral head where SZ is $\sim 50\%$ too high) and are more nearly in accordance with the calculations of Stewart and Webb,⁴ who employed a Hartree-Fock continuum wave function. These discrepancies, which arise from the different wave functions used, are most pronounced near threshold, but at higher energies ($h\nu \geq 200$ eV) the present calculation and the others mentioned differ by less than 10%.

2. Transitions $1s^2 - (2s, \epsilon p)^1P$ and $1s^2 - (2p, \epsilon s)^1P$

Calculation of the f value for photoionization and simultaneous transition to the $n=2$ state of the ion has received recent impetus since Samson¹ observed this transition and found that for a wavelength of 186.153 Å (66.003 eV) about 8% of the ions formed were excited into the $n=2$ state.

Using $(n, l) = (2, 0)$ in (3), the f values were calculated for the transition $1s^2 - (2s, \epsilon p)^1P$ and are tabulated in the third column of Table I: These re-

TABLE I. f values for transitions to $(1s, \epsilon p)^1P$, $(2s, \epsilon p)^1P$, and $(2p, \epsilon s)^1P$ states.

Excitation energy (Ry)	$(1s, \epsilon p)^1P$ state	$(2s, \epsilon p)^1P$ state	$(2p, \epsilon s)^1P$ state
0.000	1.118	9.729×10^{-3}	1.747×10^{-5}
0.250	0.9163	8.626×10^{-3}	1.648×10^{-5}
0.500	0.7389	7.391×10^{-3}	1.587×10^{-5}
0.750	0.6163	7.002×10^{-3}	1.500×10^{-5}
1.000	0.5224	6.108×10^{-3}	1.450×10^{-5}
1.58489	0.3517	4.712×10^{-3}	1.289×10^{-5}
2.51189	0.1987	3.379×10^{-3}	1.115×10^{-5}
3.98107	9.371×10^{-2}	1.802×10^{-3}	8.801×10^{-6}
6.30938	4.195×10^{-2}	8.596×10^{-4}	6.322×10^{-6}
10.000	1.424×10^{-2}	4.128×10^{-4}	3.843×10^{-6}
12.5893	7.358×10^{-3}	2.133×10^{-4}	1.449×10^{-6}
19.9526	2.134×10^{-3}	1.432×10^{-4}	1.515×10^{-6}
31.6228	5.888×10^{-4}	3.942×10^{-5}	4.747×10^{-7}
50.1185	1.463×10^{-4}	9.148×10^{-6}	1.021×10^{-7}
71.6957	4.800×10^{-5}	2.848×10^{-6}	2.671×10^{-8}
145.198	4.921×10^{-6}	2.655×10^{-7}	1.456×10^{-9}
218.700	1.267×10^{-6}	6.588×10^{-8}	2.522×10^{-10}
365.705	2.251×10^{-7}	1.134×10^{-8}	2.693×10^{-11}
549.461	5.648×10^{-8}	2.798×10^{-9}	4.498×10^{-12}
733.217	2.107×10^{-8}	1.036×10^{-9}	1.257×10^{-12}

sults are $\sim 5\%$ lower than the corresponding numbers obtained by SZ. The cross section for this transition at the spectral head (65,399 eV) is $7.848 \times 10^{-20} \text{ cm}^2$, which is consistent both with the $9 \pm 10^{-20} \text{ cm}^2$ measured by Samson and the $8.4 \times 10^{-20} \text{ cm}^2$ calculated by SZ. Further, these calculations for the ratio of the oscillator strength for transitions to $(2s, \epsilon p)^1P$ to that for transitions to $(1s, \epsilon p)^1P$ at 65,399 eV is 7.66% in agreement with Samson's data. Earlier, Carlson¹⁵ performed a similar experiment and measured the relative probability for transitions from $1s^2$ to the $n=2$ state of the residual ion and found that the ratio of the number of doubly charged to singly charged ions [i.e., $\sigma(\text{He}^{++})/\sigma(\text{He}^+)$] at 278 eV was $6 \pm 1\%$. This agrees well with the 6.7% predicted by this analysis.

The last column in Table I presents the oscillator strengths for transitions $1s^2 - (2p, \epsilon s)^1P$, that is, transitions in which the s electron is ejected leaving the residual ion in a p state. These values are 2 orders of magnitude less than the corresponding transitions in which the p electron is ejected. This result, which agrees with a general statement by Kabir and Salpeter,¹⁶ is in marked disagreement with a suggestion by Crownfield,¹⁷ who concluded from a calculation which used uncorrelated hydrogenic wave functions that the oscillator strength for the ejection of an s electron is greater than that for a p electron. Therefore, if it is possible to decide whether the ejected electron is in an s or p state by means of the angular distribution of photoelectrons,¹⁸ then this analysis supports the SZ conclusion that, for transitions to the $n=2$ state, the ejected electron will be in a p state.

3. Transitions $(1s^2) - (ns, \epsilon p)^1P (n > 2)$ and $(1s^2) - (np, \epsilon s)^1P$

In a manner precisely like that used above to calculate the cross section for simultaneous photoionization and photoexcitation to the $n=2$ state, cross sections for the transitions $(1s^2) - (ns, \epsilon p)^1P$ ($n=3-10$) and $(1s^2) - (np, \epsilon s)^1P$ ($n=2-10$) have been evaluated. These results are given in Table II as a function of the energy of the incident photon. Note that the contribution to the total photoionization cross section which transitions to these excited states make is $\sim 1.5\%$ of the ordinary photoionization cross section at low energy and $\sim 1\%$ at high energy.

Carlson¹⁵ attempted to experimentally measure the contribution of these states, but he encountered difficulty in distinguishing where transitions to higher excited states ended and where the continuum began. Nevertheless, it was found that the number of ions excited to states with $n > 2$ relative to those left in the ground state was $3 \pm 1\%$ at 278 eV, whereas this analysis predicts 1.7% of the ions will be excited to these states at the same en-

TABLE II. Helium photoionization cross sections for transitions $1s^2 - (ns, \epsilon p)^1P (n > 2)$, $1s^2 - (np, \epsilon s)^1P$.

Energy (keV)	Cross section $1s^2 - (ns, \epsilon p)^1P (n > 2)$ (cm^2)	Cross section $1s^2 - (np, \epsilon s)^1P$ (cm^2)
0.080	4.126×10^{-21}	1.270×10^{-21}
0.200	6.826×10^{-22}	2.545×10^{-22}
0.300	2.532×10^{-22}	8.543×10^{-23}
0.500	5.192×10^{-23}	8.144×10^{-24}
0.750	1.325×10^{-23}	1.577×10^{-24}
1.000	4.937×10^{-24}	4.547×10^{-25}
2.000	4.502×10^{-25}	2.323×10^{-26}
3.000	1.106×10^{-25}	3.867×10^{-27}
5.000	1.890×10^{-26}	4.083×10^{-28}

ergy.

4. Probability for Transitions to States of Quantum Number n

When simultaneous photoionization and photoexcitation can be expected to occur, it is interesting to see what percentage of the residual ions are excited into each state of principal quantum number n . Table III, which is a tabulation of the quantity

$$Q(n) = \frac{df}{d\epsilon} [(1s^2) - (ns, \epsilon p)^1P] + \frac{df}{d\epsilon} [(1s^2) - (np, \epsilon s)^1P] \\ \times \left(\sum_{n'=2}^{10} \frac{df}{d\epsilon} [(1s^2) - (n's, \epsilon p)^1P] + \frac{df}{d\epsilon} [(1s^2) - (n'p, \epsilon s)^1P] \right)^{-1}$$

(listed as a percentage) as a function of incident photon energy, illustrates the relative importance of each such excitation. Note from this table that for simultaneous photoionization and photoexcitation processes $\sim 80\%$ of the excited ions go into the $n=2$ state, and more than 95% go into one of the three lowest stages $n=2, 3$, and 4. Further, the percentage of transitions to the excited states of lower n increases as the energy of the ionizing photon increases.

5. Ejected Electron: p or s state?

As previously noted, the suggestion¹⁷ that the electron ejected in the simultaneous photoionization and photoexcitation process is more likely to be in an s rather than a p state is in conflict with previous assumptions.^{5, 16} Although this suggestion came from a calculation using uncorrelated hydrogenic wave functions and is not otherwise supported, it is nevertheless of interest to apply the general approach outlined in Sec. II to resolve whatever doubt remains. To this end, the f values for both the transitions $(1s^2) - (ns, \epsilon p)^1P$ and $(1s^2) - (np, \epsilon s)^1P$ have been calculated, and the ratio

TABLE III. Simultaneous photoionization and photoexcitation probability of excitation to state n (%).

Energy (keV)	Q(2)	Q(3)	Q(4)	Q(5)	Q(6)	Q(7)	Q(8)	Q(9)	Q(10)
0.080	77.702	12.71	4.519	2.133	1.182	0.727	0.481	0.335	0.242
0.200	78.590	12.249	4.300	2.030	1.126	0.693	0.458	0.319	0.231
0.300	79.494	11.791	4.089	1.930	1.072	0.660	0.436	0.304	0.220
0.500	80.662	11.221	3.825	1.795	0.999	0.611	0.404	0.218	0.204
1.000	81.751	10.707	3.580	1.666	0.918	0.563	0.370	0.257	0.186
5.000	82.767	10.231	3.353	1.544	0.846	0.516	0.338	0.234	0.169

$$Y(n) = \frac{df}{d\epsilon} [(1s^2)-(np, \epsilon s)^1P] / \frac{df}{d\epsilon} [(1s^2)-(ns, \epsilon p)^1P] \quad (6)$$

has been tabulated for $n=2-10$ as a function of incident photon energy in Table IV.

From this table it can be observed that the probability for ejecting an s electron (leaving the residual ion in a p state) increases with increasing n relative to that for ejection of a p electron: At 200 eV, the ratio (6) is $\sim 26\%$ for $n=3$, and it is $\sim 73\%$ for $n=10$. Also, for any particular n , this ratio increases as the energy of the incident photon decreases.

The last column in Table IV is the sum

$$\sum_{n=2}^{10} \left(\frac{df}{d\epsilon} [(1s^2)-(np, \epsilon s)^1P] \right) / \sum_{n=2}^{10} \left(\frac{df}{d\epsilon} [(1s^2)-(ns, \epsilon p)^1P] \right),$$

which illustrates the conclusion that for transitions involving photo-ionization and photoexcitation to all allowed states (truncated at $n=10$), the ratio of the probability that the photoelectron will be in a p state to that for it to be in an s state is less than 10% near threshold, and this ratio decreases, at higher energies.

Using Tables I – IV together, the cross section for transitions from the ground $1s^2$ state of helium to any allowed excited state of the He^+ ion ($n \leq 10$) may be derived. The contribution that the cross section for simultaneous photoionization and photoexcitation (to all allowed states considered) makes to the ordinary photoionization cross section, where

the residual ion is left in the ground state, is found to be $\sim 9\%$ for photon energies $\sim 80-400$ eV, and for higher energies this contribution asymptotically approaches $\sim 7\%$.

IV. DISCUSSION

When the energy of the incident photon is in excess of the helium double-ionization threshold (79 eV), then the photoionization cross section includes three contributions: (i) $(1s^2)-(1s, \epsilon p)^1P$ transitions in which the residual ion remains in the ground state; (ii) simultaneous photoionization and photoexcitation; and (iii) double ionization. (i) and (ii) have been evaluated in this paper, and the double-ionization cross section has been measured experimentally¹⁵ and calculated elsewhere.^{8, 19} Inclusion of the contributions from (ii) and (iii) in the ordinary photoionization cross section [(i)] has the effect of increasing the helium photoionization cross section by $\sim 12\%$ at low energies (80 eV $\leq \hbar\omega \leq 400$ eV) and by $\sim 10\%$ at higher photon energies. Let us inquire whether the effect of this increase can be measured.

The experimental method used to measure cross sections consists of exciting atomic x-ray lines and then passing this radiation through a container of helium gas for a specific time. Having traversed the gas, the photons are registered on a photographic plate. The container is then evacuated and the experiment repeated for the same length of time; by measuring the density of the lines on the exposed plates, one has a measure of $\log(I/I_0)$ which is

TABLE IV. Simultaneous photoionization and photoexcitation: probability of excitation to bound np states (%).

Energy (keV)	Y(2)	Y(3)	Y(4)	Y(5)	Y(6)	Y(7)	Y(8)	Y(9)	Y(10)	Sum
0.080	0.112	31.037	51.251	63.050	70.983	76.780	81.237	84.789	87.611	9.826
0.200	0.354	25.932	42.808	52.665	59.284	64.120	67.843	70.803	73.150	6.252
0.300	1.058	14.182	22.089	26.636	29.634	31.789	33.384	34.691	35.201	4.267
0.500	1.276	7.494	11.394	13.739	15.314	16.459	17.311	17.983	18.519	2.838
1.000	0.938	3.666	5.533	6.708	7.513	8.100	8.543	8.893	9.172	1.628
5.000	0.237	0.764	1.151	1.402	1.576	1.704	1.801	1.878	1.939	0.370

proportional to the atomic absorption coefficient. Obviously, if the energy of the ionizing radiation is greater than 5.8 Ry, the measured cross section is not that corresponding to transitions $(1s^2)-(1s, \epsilon p)^1P$ alone, but it also includes transitions to all the doubly excited states mentioned above.

When previous calculations of the helium photoionization cross section (which considered only ordinary photoionization) were compared with the experimental data, it was found that the agreement was excellent near threshold, but that deviations appeared at higher energies ($\hbar\omega \gtrsim 12$ Ry), with the result that the measured points were preferentially larger than the calculations.⁶ It has been assumed that this discrepancy was attributable to experimental errors owing to the inherently small cross sections at high energies and the presence of contaminants, especially of nitrogen and carbon dioxide, which tend to make the cross section unrealistically large. However, if transitions to doubly excited states are included, the agreement improves substantially.

The helium photoionization cross section, including the contributions from simultaneous photoionization and photoexcitation calculated here and from double ionization,¹⁹ has been used to obtain the

quantity $(\hbar\omega)^3 df/d\epsilon$, which is plotted on Fig. 1 as a function of the energy of the incident photon. The experimental data²⁰⁻²² obtained by application of the method described above are also plotted on this figure for comparison. Note that good agreement is obtained at low energies, but that at higher energies ($\hbar\omega \gtrsim 12$ Ry) the measured points lie preferentially above the calculation by $\sim 5\%$, although the data of different groups show some scatter.

When the results of other calculations are compared with these data, the discrepancies at the higher energies become quite large. For example, at 20.6 Ry both Bell and Kingston's⁶ momentum and position cross sections fall well below the measured points which are quoted with errors of $\pm 10\%$. It is concluded that the theoretical helium photoionization cross section becomes more compatible with experimental data if the total cross section includes the contribution from simultaneous photoionization and photoexcitation and that from double ionization.

ACKNOWLEDGMENT

I am grateful to Professor R. J. Gould for valuable suggestions and critical comment.

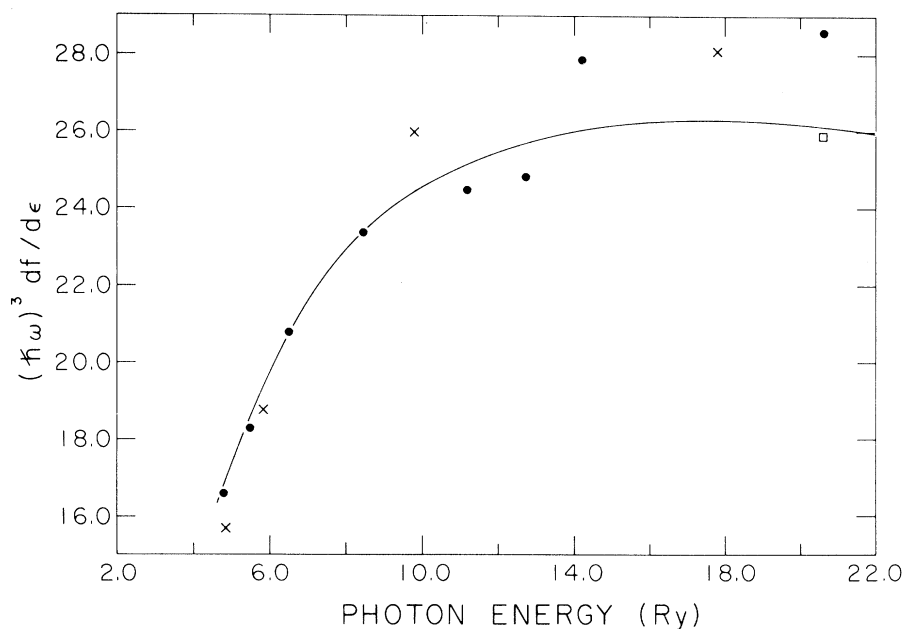


FIG. 1. $(I + \epsilon)df/d\epsilon$ including contributions from doubly excited (bound-free) states. The experimental data of Lukirskii *et al.* (dot), Lowry *et al.* (cross), and Dersham and Schein (square) are noted.

[†]Work carried out at the University of California at San Diego under grants from the National Science Foundation and the National Aeronautics and Space Administration.

*Operated by Associated Universities, Inc., under contract with the National Science Foundation.

¹J. A. R. Samson, *Phys. Rev. Letters*, **22**, 693 (1969).

²J. P. Vinti, *Phys. Rev.* **42**, 632 (1932).

³J. A. Wheeler, *Phys. Rev.* **43**, 258 (1933).

⁴A. L. Stewart and T. G. Webb, *Proc. Phys. Soc. (London)* **82**, 532 (1963).

⁵E. E. Salpeter and M. H. Zaidi, *Phys. Rev.* **125**, 248 (1962).

⁶K. L. Bell and A. E. Kingston, *Proc. Phys. Soc.*

(London) 90, 31 (1967).

⁷A. Dalgarno and A. L. Stewart, Proc. Phys. Soc. (London) 76, 49 (1960).

⁸F. W. Byron, Jr., and C. J. Joachain, Phys. Rev. 164, 1 (1967). This wave function will subsequently be denoted by BJ.

⁹The idea that the correlated BJ wave function would be useful for calculating "double-excitation (bound-free)" cross sections was implied in the authors's paper, Ref. 8.

¹⁰Atomic units with energies in rydbergs are used throughout.

¹¹H. Bethe and E. E. Salpeter, The Quantum Mechanics of One- and Two-Electron Atoms (Academic Press Inc., New York, 1957).

¹²R. L. Brown, Ph. D. thesis, University of California, San Diego, 1969 (unpublished).

¹³W. Gordon, Ann. Phys. (Paris) 2, 1031 (1929).

¹⁴L. C. Biedenharn, J. L. McHale, and R. M. Thaler,

Phys. Rev. 100, 376 (1955).

¹⁵T. A. Carlson, Phys. Rev. 156, 142 (1966).

¹⁶P. K. Kabir and E. E. Salpeter, Phys. Rev. 108, 1256 (1957).

¹⁷F. R. Crownfield, in Fifth International Conference on the Physics of Electronic and Atomic Collisions, (Leningrad Nauka Publishing House, Leningrad, U. S. S. R., 1967), p. 621.

¹⁸J. A. R. Samson, Proceedings of a Symposium on Photo-Electron Spectroscopy Report, London, 1969 (unpublished).

¹⁹R. L. Brown, Phys. Rev. (to be published).

²⁰J. F. Lowry, D. H. Tomboulion, and E. L. Ederer, Phys. Rev. 137, A1054 (1965).

²¹A. P. Lukirskii, I. A. Brytov, and T. M. Zimkina, Opt. i Spectroskopia [English transl.: Opt. Spectry. 17, 234 (1964)].

²²E. Dershman and M. Schein, Phys. Rev. 37, 1238 (1931).

Particle-Surface-Wave Coupling in a He³ Film*

Peter J. Feibelman[†]

Centre d'Etudes Nucléaires de Saclay, B.P. No. 2, 91, Gif-Sur-Yvette, France

(Received 13 December 1969)

We study the coupling of the surface oscillations of a free He³ film to the He³ particles of which the film is composed. A check on the self-consistency of the lowest-order theory of this coupling fails because of an infrared divergence. We, therefore, are led to use exact dynamical equations and find that the infrared difficulty then disappears because the exact theory takes the classical Maxwellian distribution of surface vibration properly into account. The resulting form of the coupling may be used to study the possibility of a superfluid pairing transition in a free He³ film.

I. INTRODUCTION

In a previous publication,¹ we have shown that a free He³ film, i.e., one without a solid substrate such as a soap bubble, will support surface vibrations. These are simply drumhead oscillations. The presence of such excitations of the film may lead to interesting physical phenomena, for example, a superfluid pairing transition. Thus, it is important to estimate the strength of interaction between He³ particles induced by the exchange of a surface wave.

The lowest-order theory of the surface wave is based on the random-phase approximation (RPA). In this approximation, the single-particle states are simply Hartree states. In Sec. II of this pa-

per, we exhibit this lowest-order theory, and observe that it cannot be a consistent one, since our estimate of the correction to the self-energy of the single-particle states due to the emission and re-absorption of surface waves diverges logarithmically as the surface area of the film becomes infinitely large.

In the exact dynamical theory described qualitatively in Sec. III and mathematically in Sec. IV, the coupling of He³ particles to surface waves is reduced as a result of the smearing of the surface due to the film's thermal vibration. This smearing effect exactly cancels the divergences of the lowest-order theory. Thus, we obtain a well-behaved particle-surface-wave coupling and open the possibility of looking for a superfluid phase transition of the film.